JOURNAL OF PROPULSION AND POWER
Vol. 12, No. 4, July–August 1996

Breakup of Annular Viscous Liquid Jets in Two Gas Streams

Jihua Shen* and Xianguo Li†
University of Victoria, Victoria, British Columbia V8W 3P6, Canada

Linear stability theory is applied to study the breakup process of an annular viscous liquid jet exposed to both inner and outer gas streams of unequal velocities. The absolute liquid and gas velocities are considered in this temporal instability analysis. It is found that not only the velocity difference across each interface, but also the absolute velocity of each fluid is important for the jet instability, although the effect of absolute velocity is secondary compared with that of relative velocity. A high-velocity co-flowing gas stream is found to significantly improve atomization performance. A high-velocity gas inside of the annular liquid jet promotes the jet breakup process more than the gas of equivalent velocity outside of the jet. For equal liquid and gas velocities, surface tension, liquid, and gas density exhibit effects on wave growth rates different from those when a velocity discontinuity is present across interfaces. However, the viscous damping effect on jet instability always exists for the cases with and without velocity differences at high Weber numbers. The liquid inertia, density ratio, and high gas velocity all contribute to better atomization performance, whereas surface tension and liquid viscosity increase the resulting droplet size.

Nomenclature

a = dimensionless inner radius, a^*/h
a^* = inner radius of annular sheet, m
b = dimensionless outer radius, b^*/h; $a + 2$
b^* = outer radius of annular sheet, m
h = reference length scale, m, $(b^* - a^*)/2$
I_0, I_1 = modified Bessel function of the first kind of order 0 and 1
i = imaginary number, $\sqrt{-1}$
K_0, K_1 = modified Bessel function of the second kind of order 0 and 1
k = dimensionless wave number, αh
P, $\bar{P}$ = pressure of perturbed and base flow, N/m^2
p = pressure change induced by perturbation, N/m^2
$\tilde{p}$ = initial amplitude of pressure p, N/m^2
Re = Reynolds number, $U_{ij}^* h/\nu_{ij}$
t = time, s
U = dimensionless axial velocity of base flow, U^*/U_{ij}^*
U^* = axial velocity of base flow, m/s
$\boldsymbol{U}$, $\bar{\boldsymbol{U}}$ = velocity vector of perturbed and base flow, m/s
$\boldsymbol{u}$ = change of velocity vector induced by perturbation, m/s
$\tilde{\boldsymbol{u}}$ = initial amplitude of velocity $\boldsymbol{u}$, m/s
We = Weber number, $\rho_{ij} U_{ij}^{*2} h/\sigma$
α = wave number, 1/m
ε = initial amplitude of disturbance, m
η = displacement of interface from its initial equilibrium position, m
λ = wavelength, m, $2\pi/\alpha$
μ = dynamic viscosity, kg/m·s
ν = kinematic viscosity, m^2/s
ρ = density ratio, ρ_g/ρ_{lj}
ρ_n = density, kg/m^3
σ = surface tension, N/m
Ω = wave frequency, 1/s
ω = dimensionless wave frequency, $\Omega h/U_{ij}^*$

Subscripts
g = both inner and outer gas medium
i = imaginary part of a complex variable
ig = inner gas medium or at inner interface
lj = liquid jet
n = g, lj
og = outer gas medium or at outer interface
r = real part of a complex variable

Received June 24, 1995; presented as Paper 95-3121 at the AIAA/ASME/SAE/ASEE 31st Joint Propulsion Conference and Exhibit, San Diego, CA, July 10–12, 1995; revision received Dec. 18, 1995; accepted for publication Jan. 6, 1996.

*Graduate Student, Department of Mechanical Engineering.
†Associate Professor, Department of Mechanical Engineering. Member AIAA.

Introduction

THE breakup process of an annular liquid jet (or sheet) in moving gas streams is of practical significance for twin-fluid, such as air-assist or air-blast, atomization. By exposing a relatively slow-moving liquid sheet to high-velocity air (or gas) streams, the growth of disturbances at the gas–liquid interfaces is enhanced to cause the liquid jet to breakup more rapidly into ligaments and then droplets, forming a spray.[1] The rate of disturbance amplification is mainly because of the complex influence of surface tension force and aerodynamic interaction between the liquid and gas phases. This type of liquid atomization process is widely used in many practical power generation and propulsion systems. However, the fundamental understanding of the mechanism of atomization is still far from complete. The primary objective of this work is to investigate the fundamental mechanism of the interfacial instability of an annular viscous liquid jet subject to both inner and outer gas streams of unequal velocities.

Some works have been carried out to study the breakup process of an annular liquid jet. Crapper et al.[2] analyzed theoretically the instability of an inviscid annular liquid sheet moving in an inviscid stationary gas medium. The temporal wave growth rates were obtained for two unstable wave modes, paravaricose (symmetric) and parasinuous (antisymmetric), with the approximation of very thin liquid sheets. Meyer and Weihs[3] investigated the capillary instability of a static viscous liquid sheet in a moving gas stream with a particular type of disturbance by assuming the amplitude ratio of initial disturbances at the outer interface to that at the inner interface is equal to the ratio of the inner-to-outer radii of the jet. The instability of a stationary viscous annular liquid sheet with unequal gas velocities for the inner and outer gas streams

was formulated by Lee and Chen.[4] Two dispersion relations corresponding to each interface were derived. However, only cases for inviscid liquids were examined in their study.

Recently, a temporal instability analysis was carried out for an annular viscous liquid jet moving in an inviscid gas medium at rest.[5] Three limiting cases of a round liquid jet, a gas jet, and a plane liquid sheet were recovered with appropriate geometric approximations to the annular jet. It was found that the parasinuous mode of unstable waves outgrows the paravaricose mode at large Weber numbers of practical importance as in liquid atomization. Here, the Weber number is defined as the ratio of liquid inertial force to capillary force. Liquid viscosity has a complicated dual effect on the jet instability. For a thin annular liquid sheet at low Weber numbers, liquid viscosity destabilizes an additional range of wave numbers beyond those corresponding to the aerodynamic instability, and may even become dominant under certain flow conditions, very similar to a thin plane liquid sheet.[6] For most practical applications where the Weber number is usually large, liquid viscosity reduces the jet instability. It was also found that the presence of an ambient gas always promotes the breakup process of the jet when there is a velocity discontinuity across liquid–gas interfaces, and there exists a critical Weber number below which surface tension is a source of instability. Whereas above it, aerodynamic interaction between the liquid and gas phases promotes the instability development, and surface tension has a stabilizing effect on the jet. This is similar to the breakup of a round liquid jet,[7] where the surface tension has dual effects-destabilizing in the Rayleigh breakup regime and stabilizing in the atomization regime. However, as will be shown later, both gas-to-liquid density ratio and surface tension have different effects on the jet instability when the gas and liquid velocities are equal, as compared with the case of a moving liquid jet in a stationary gas medium.

As mentioned earlier, in twin-fluid atomization a high-velocity gas stream is often utilized to promote the breakup of liquid jets and enhance significantly the mixing of liquid with gas. The experiments for plane liquid sheets exposed to high velocity coflowing gas streams,[8,9] and for an annular liquid sheet subject to only inner gas stream,[4,10] indicate that using high-velocity gas on one or both sides of liquid sheets enhances considerably the breakup processes of the liquid sheets. However, in all of the existing theoretical studies,[2–4] either stationary liquid or gas is considered. This study attempts to examine the effect of unequal inner and outer gas velocities on an annular jet breakup process. Since the Galilean transformation of coordinate often changes the characteristics of the temporal–spatial evolution of unstable waves,[11,12] the absolute velocities of both liquid and gas phases should be taken into account, as Li did in a temporal instability analysis of a plane liquid sheet in gas streams of unequal velocities.[13] He found that at high Weber numbers, it is the velocity difference across each interface that determines the temporal wave growth rate rather than the absolute velocities. However, at low Weber numbers, it is the absolute value of liquid and gas velocity, rather than the relative velocity, that controls the instability process. For an annular liquid jet, because of the different curvatures of two interfaces, the same gas stream applied to the inner interface has a different effect on the jet instability than that at the outer interface, as shall be shown later.

In this study, a linear instability analysis has been carried out for an annular viscous liquid jet moving in gas streams of unequal velocities. The dispersion relation and the amplitude ratio of initial disturbances at the two interfaces are derived, and results are presented for temporal mode of unstable waves. The effects of various inner and/or outer gas velocities and coflowing gas streams are examined under the given flow conditions (Reynolds number, Weber number, and gas-to-liquid density ratio). The effects of gas-to-liquid density ratio, liquid viscosity, and surface tension are also investigated with and without a velocity discontinuity across the liquid–gas interfaces.

Instability Analysis

Small disturbances are assumed in the derivation of the dispersion relation and the equation for the amplitude ratio of initial disturbances at two gas–liquid interfaces by considering unequal gas velocities on both sides of an annular viscous liquid jet. As shown in Fig. 1, the annular jet is assumed semi-infinitely long and with inner radius a^*, outer radius b^*, constant density ρ_{lj}, and viscosity μ_{lj}. The jet moves at a uniform axial velocity U_{lj}^* with its two sides exposed to inviscid gas streams of velocity U_{ig}^* inside of the jet and U_{og}^* outside of the jet. The gas density is denoted by ρ_g. Both gas and liquid velocities are presumed to be small compared with the velocity of sound. Therefore, both gas and liquid can be considered incompressible. Furthermore, gravity is neglected. The pressure field is constant within the liquid and gas phases, respectively, and it has a jump across the two liquid–gas interfaces, because of the effect of σ. When disturbances set in, resulting in the interface deformation and deviation away from the equilibrium configuration of the annular liquid jet, the flowfield is disturbed with the perturbed flow velocity $\boldsymbol{u}$ and pressure p superimposed on the base flow velocity $\bar{\boldsymbol{U}}$ and pressure $\bar{P}$. Then, in a cylindrical coordinate system (z, r, θ), the perturbed flowfields become

$$\boldsymbol{U}_n = \bar{\boldsymbol{U}}_n + \boldsymbol{u}_n, \qquad \boldsymbol{u}_n = (u_n, v_n, 0), \qquad P_n = \bar{P}_n + p_n \tag{1}$$

where the subscript n = lj, ig, and og corresponds to the liquid jet, the inner, and outer gas streams, respectively. The base flow quantities are given by

$$\bar{\boldsymbol{U}}_{lj} = (U_{lj}^*, 0, 0), \qquad \bar{\boldsymbol{U}}_{ig} = (U_{ig}^*, 0, 0), \qquad \bar{\boldsymbol{U}}_{og} = (U_{og}^*, 0, 0)$$

$$\bar{P}_{lj} = \bar{P}_{ig} - \sigma/a^* = \bar{P}_{og} + \sigma/b^*$$

The equations governing the motion of the perturbed flow are the conservation of mass and momentum, which become, upon linearization,

$$\nabla \cdot \boldsymbol{u}_n = 0 \tag{2}$$

$$\rho_n \left(\frac{\partial}{\partial t} + U_n^* \frac{\partial}{\partial z} \right) \boldsymbol{u}_n = -\nabla p_n + \mu_n \nabla^2 \boldsymbol{u}_n \tag{3}$$

The boundary conditions that the solutions of the previous governing equations have to satisfy are the kinematic and dynamic conditions at the inner and outer interfaces, which are represented by $r = a^* + \eta_{ig}(z, t)$ and $r = b^* + \eta_{og}(z, t)$, respectively. In linear stability theory, these conditions need not be applied at the disturbed liquid–gas interfaces. Rather, they can be linearized in the same manner as done previously for the governing equations. Then the linearized boundary conditions can be applied at the unperturbed interfaces. Because the interfaces are material surfaces, the kinematic boundary conditions at $r = a^*$ and $r = b^*$ are, respectively,

$$v_{lj} = \frac{\partial \eta_{ig}}{\partial t} + U_{lj}^* \frac{\partial \eta_{ig}}{\partial z} \quad \text{and} \quad v_{lj} = \frac{\partial \eta_{og}}{\partial t} + U_{lj}^* \frac{\partial \eta_{og}}{\partial z} \tag{4}$$

$$v_{ig} = \frac{\partial \eta_{ig}}{\partial t} + U_{ig}^* \frac{\partial \eta_{ig}}{\partial z} \quad \text{and} \quad v_{og} = \frac{\partial \eta_{og}}{\partial t} + U_{og}^* \frac{\partial \eta_{og}}{\partial z} \tag{5}$$

The dynamic condition implies that the shear stress must vanish at the interfaces because of the inviscid assumption for the gas phase, and normal stresses across the interfaces must

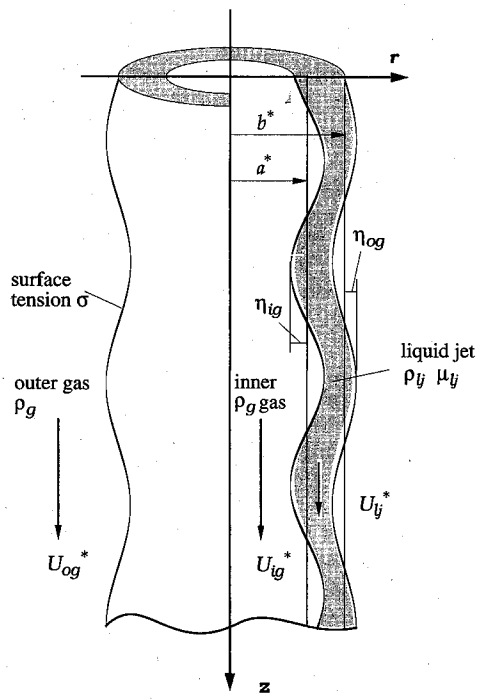

Fig. 1 Schematic of annular liquid jet.

be continuous with allowance for the effect of σ. Mathematically, these conditions can be expressed as follows:

$$\mu_{lj}\left(\frac{\partial u_{lj}}{\partial r}+\frac{\partial v_{lj}}{\partial z}\right)=0 \quad (\text{at } r=a^* \text{ and } r=b^*) \tag{6}$$

$$p_{ig}-p_{lj}+2\mu_{lj}\frac{\partial v_{lj}}{\partial r}=-\sigma\left(\frac{\eta_{ig}}{a^{*2}}+\frac{\partial^2\eta_{ig}}{\partial z^2}\right) \quad (\text{at } r=a^*) \tag{7}$$

$$p_{og}-p_{lj}+2\mu_{lj}\frac{\partial v_{lj}}{\partial r}=\sigma\left(\frac{\eta_{og}}{b^{*2}}+\frac{\partial^2\eta_{og}}{\partial z^2}\right) \quad (\text{at } r=b^*) \tag{8}$$

Further, in the ambient gas phase, the effects of disturbances should physically remain bounded, whether it is at the centerline or far away from the liquid jet. That is,

$$\boldsymbol{u}_{ig} \text{ and } p_{ig} \text{ bounded as } r\to 0 \tag{9}$$

$$\boldsymbol{u}_{og} \text{ and } p_{og} \text{ bounded as } r\to\infty \tag{10}$$

The solutions to the governing equations are sought in terms of the normal mode in the following form:

$$(\boldsymbol{u}_n, p_n, \eta_{ig}, \eta_{og})=[\tilde{\boldsymbol{u}}_n(r), \tilde{p}_n(r), \varepsilon_{ig}, \varepsilon_{og}]\exp(\Omega t+i\alpha z) \tag{11}$$

where n = lj, ig, and og, ε_{ig} and ε_{og} are the amplitudes of initial disturbances at the inner and outer interfaces, and are regarded to be much smaller than the inner and outer radius as well as the thickness of the annular liquid jet. The axial wave number of the disturbance α is related to the disturbance wavelength λ by the relation $\alpha=2\pi/\lambda$. The complex frequency Ω has a real and imaginary part. The real part Ω_r represents the rate of growth or decay of the disturbance with time, the imaginary part Ω_i is equal to 2π times of the disturbance frequency, and $-\Omega_i/k$ represents the wave propagation velocity of the disturbance.

Substituting Eq. (11) into the governing differential equations [Eqs. (2) and (3)], yields the required general solution with a set of unknown integration constants, which can be determined by the boundary conditions [Eqs. (4–6), (9), and (10)]. Then, the balance of normal stresses at the two interfaces, Eqs. (7) and (8), leads to the following dispersion relation between the complex eigenfrequency and disturbance wave number, in dimensionless form:

$$\begin{aligned}&\left\{(l^2+k^2)^2\Delta_1\Delta_4+4k^3l\Delta_3\Delta_6+\left[\frac{k}{We}\left(\frac{1}{a^2}-k^2\right)\right.\right.\\&\left.\left.-\rho(\omega+ikU_{ig})^2\frac{I_0(ka)}{I_1(ka)}\right]Re^2-\frac{2k}{a}Re(\omega+ik)\right\}\\&\times\left\{(l^2+k^2)^2\Delta_2\Delta_4-4k^3l\Delta_3\Delta_5+\left[\frac{k}{We}\left(\frac{1}{b^2}-k^2\right)\right.\right.\\&\left.\left.-\rho(\omega+ikU_{og})^2\frac{K_0(kb)}{K_1(kb)}\right]Re^2+\frac{2k}{b}Re(\omega+ik)\right\}\\&-\frac{1}{ab}\left[\frac{(l^2+k^2)^2}{k}\Delta_4-4k^3\Delta_3\right]^2=0\end{aligned} \tag{12}$$

As a part of the solution, the amplitude ratio of the initial disturbances at the inner and outer interfaces becomes

$$\frac{\varepsilon_{ig}}{\varepsilon_{og}}=-\frac{(l^2+k^2)^2\Delta_4/k-4k^3\Delta_3}{a[(l^2+k^2)^2\Delta_1\Delta_4+4k^3l\Delta_3\Delta_6-(2k/a)\mathrm{Re}(\omega+ik)+B_{ig}]} \tag{13}$$

or

$$\frac{\varepsilon_{og}}{\varepsilon_{ig}}=-\frac{(l^2+k^2)^2\Delta_4/k-4k^3\Delta_3}{b[(l^2+k^2)^2\Delta_2\Delta_4-4k^3l\Delta_3\Delta_5-(2k/b)\mathrm{Re}(\omega+ik)+B_{og}]} \tag{14}$$

where

$$B_{ig}=Re^2\left[\frac{k}{We}\left(\frac{1}{a^2}-k^2\right)-\rho(\omega+ikU_{ig})^2\frac{I_0(ka)}{I_1(ka)}\right]$$

$$B_{og}=Re^2\left[\frac{k}{We}\left(\frac{1}{b^2}-k^2\right)-\rho(\omega+ikU_{og})^2\frac{K_0(kb)}{K_1(kb)}\right]$$

$$l=\sqrt{k^2+Re(\omega+ik)}$$

$$\Delta_1=I_0(ka)K_1(kb)+K_0(ka)I_1(kb)$$

$$\Delta_2=I_0(kb)K_1(ka)+K_0(kb)I_1(ka)$$

$$\Delta_3=[I_1(la)K_1(lb)-I_1(lb)K_1(la)]^{-1}$$

$$\Delta_4=[I_1(ka)K_1(kb)-I_1(kb)K_1(ka)]^{-1}$$

$$\Delta_5=[I_0(lb)K_1(la)+K_0(lb)I_1(la)]$$

$$\Delta_6=-[I_0(la)K_1(lb)+K_0(la)I_1(lb)]$$

Results and Discussion

The temporal linear instability analysis is carried out to examine the effects of various inner U_{ig} and/or outer gas velocities U_{og}, as well as fluid properties on the jet instability. By using Muller's method,[14] the dispersion relation [Eq. (12)] is solved for temporal modes of unstable wave growth rate ω_r, the positive real part of complex wave frequency representing the degree of jet instability. Similar to our earlier study of liquid jets in stationary gas medium,[5] two families of unstable solutions, parasinuous and paravaricose, are obtained. The results shown here are all for a fixed nozzle geometry of a = 40.12 (and, hence, b = 42.12), which corresponds to an annular nozzle of $2a^*=9.525\times10^{-3}$ m and $2b^*=10\times10^{-3}$ m used in the experiment of a water–air system in our laboratory.

These nozzle dimensions are comparable with those of other recent studies, such as that of Ramamurthi and Tharakan.[15]

Effects of Inner and Outer Gas Velocities

Figure 2 shows ω_r for different velocities of U_{ig} with stationary outer gas medium ($U_{og} = 0$). It is seen from Fig. 2a that the growth rate for parasinuous disturbances decreases along with the dominant wave number as the inner gas velocity increases from 0 to 1, or the velocity difference ($\Delta U_{ig} = |U_{ig} - 1|$) between the gas and liquid phases as the inner interface decreases from 1 to 0. Further increase in U_{ig} up to 2 causes ω_r to increase, since the velocity difference ΔU_{ig} increases from 0 to 1. The unstable wave number range does not change significantly for $0 \leq U_{ig} \leq 2$. When U_{ig} is larger than 2, ω_r increases considerably while the dominant wave number increases relatively slowly. Clearly, the velocity difference across the interface enhances the jet instability and extends the unstable wave regime to higher wave numbers. However, it is seen that the growth rate at a higher gas velocity (e.g., $U_{ig} = 1.7$) is larger than that at a lower one (e.g., $U_{ig} = 0.3$), even though the velocity difference across each interface is the same. Hence, it indicates that not only the velocity difference across each interface, but also the absolute gas and liquid velocity themselves affect the breakup processes of annular liquid jets. Calculations of disturbance energy, similar to that of Li[13] and Lin and Creighton,[17] implies that a shift in the disturbance frequency and phase angle of gas pressure fluctuations[6] is responsible for this behavior.

As for the paravaricose mode (Fig. 2b), ω_r also increases with ΔU_{ig}, but approaches a certain limit. This indicates that when the gas velocity is sufficiently large, a further increase in the gas velocity has little effect on the growth rate of the paravaricose mode. This is because the paravaricose mode, as shown by Li[13] for plane liquid sheets, is always related primarily with the smaller of the two velocity differences across the two interfaces, whereas the parasinuous mode is always associated with the larger velocity difference across the interfaces. It is also seen from Fig. 2 that the unstable wave growth rate for the parasinuous mode is approximately two orders of magnitude larger than that for the corresponding paravaricose mode, indicating that, in practice, the parasinuous unstable waves will outgrow paravaricose ones and predominate the jet breakup processes. However, it is known that the paravaricose mode becomes more important as the gas-to-liquid density ratio ρ increases. As Rangel and Sirignano[16] show for a plane liquid sheet, the growth rates for both modes become comparable at $\rho = 0.25$, and the paravaricose mode becomes dominant at $\rho = 1$. For the present problem, the parasinuous mode has a much larger growth rate than the corresponding paravaricose mode for the density ratio up to about 0.1, which corresponds to the conditions in rocket engines and is probably the highest density ratio that may be encountered in practical applications. Therefore, only parasinuous solutions will hereafter be presented.

When the inner gas stream is stationary ($U_{ig} = 0$), but U_{og} is varied, ω_r exhibits the same trends as discussed previously. The comparison of these two sets of parasinuous growth rates are shown in Fig. 3 at low and high gas velocities, respectively. At low gas velocities ($U_{ig} \leq 2$ or $U_{og} \leq 2$), it is seen from Fig. 3a that ω_r, shown by the dashed curves for $U_{ig} = 0$, is larger than that given by the solid curves for $U_{og} = 0$ for a comparable gas velocity on the other side of the liquid jet. For either $U_{ig} \geq 2$ or $U_{og} \geq 2$ and the gas on the other side of the liquid jet stationary, Fig. 3b shows that ω_r for $U_{og} = 0$ is larger than that for $U_{ig} = 0$. From both Figs. 3a and 3b, it is seen that the larger wave growth rate always occurs when the velocity difference across the inner surface ($\Delta U_{ig} = |U_{ig} - 1|$) is larger than that across the outer interface ($\Delta U_{og} = |U_{og} -$

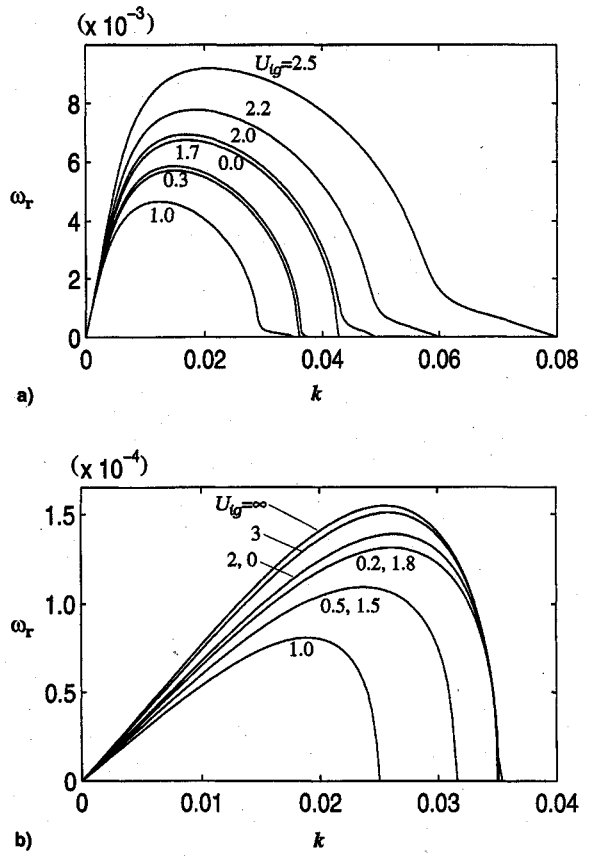

Fig. 2 Wave growth rate for different velocities of inner gas stream with stationary outer gas medium. a = 40.12, Re = 4112, We = 19.25, ρ = 0.00129, and U_{og} = 0: a) parasinuous and b) paravaricose mode.

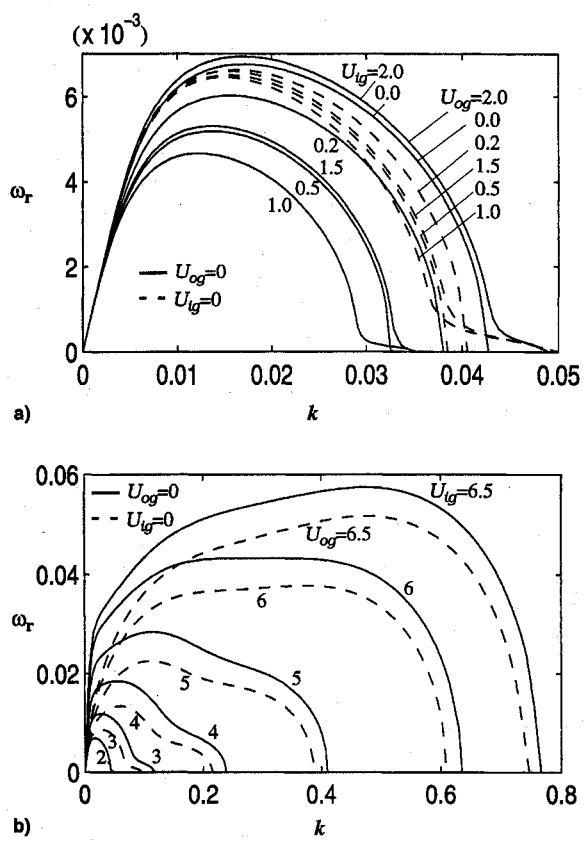

Fig. 3 Wave growth rate of the parasinuous mode for different velocities of gas stream on either inner or outer side of the jet. a = 40.12, Re = 4112, We = 19.25, and ρ = 0.00129: a) low and b) high gas velocity.

1|). This implies that to promote jet instability, a gas stream applied to the outer interface is more effective than when applied to the inner surface when the gas velocity is less than twice the liquid velocity, whereas the gas stream with a velocity higher than twice the liquid velocity should be exposed to the inner interface. This may explain why the airstream in practical air-assisted atomization is sometimes supplied inside of the liquid jet, and sometimes outside of the jet. It is also interesting to see from Fig. 3b that the tailing portion of the growth rate curve at higher wave numbers increases with the gas velocity, and exceeds the leading portion at lower wave numbers when the gas velocity is approximately higher than 6. This indicates that the dominant wavelength may not decrease smoothly with the gas velocity, rather it may have a sudden decrease under certain flow conditions, e.g., at U_a of about 6 for the present case. Therefore, the corresponding drop size may suddenly decrease significantly as the gas velocity is gradually increased.

The initial amplitude ratio shown in Fig. 4, calculated from Eqs. (13) or (14) under the same conditions as those for the wave growth rate in Fig. 3, shows that at larger wave numbers, the initial amplitude at the inner interface ε_{ig} is larger than that at the outer interface ε_{og} for $U_{ig} > U_{og}$, whereas ε_{og} is larger than ε_{ig} for $U_{og} > U_{ig}$. This implies that the larger initial amplitude occurs at the interface that is subject to a gas stream of higher velocity compared with the other side of the jet for short waves. Note that this result is obtained for the case where only one interface is exposed to a moving gas stream. At smaller wave numbers, the initial amplitude ratio ($\varepsilon_{ig}/\varepsilon_{og}$) or ($\varepsilon_{og}/\varepsilon_{ig}$) approaches a fixed value,[5] which is the limit of Eq. (13) as the wave number $k \to 0$:

$$\frac{\varepsilon_{ig}}{\varepsilon_{og}} \to \frac{b}{a}\frac{1}{[1-\rho(1-b^2/a^2)]}$$

When the gas-to-liquid density ratio is much smaller than 1 and (b/a) is of order of 1, ($\varepsilon_{ig}/\varepsilon_{og}$) approaches ($b/a$), i.e., 1.05 for the present case.

To examine the effect of a coflowing gas stream on the jet breakup process, the parasinuous wave growth rate is shown in Fig. 5, for various gas velocities on both sides of the liquid jet. For comparison, the growth rate from a single gas stream on the inner side of the sheet is also shown in Fig. 5. It is obvious from Fig. 5a that the coflowing gas stream increases the wave growth rate significantly as compared with a single gas stream. It especially shifts the dominant wave to shorter wavelengths. This indicates that using coflowing air in air-assisted atomization is beneficial for the improvement of the atomization performance compared with a single airstream when the air velocity is at least three or four times larger than the liquid velocity (Fig. 5a). When the dimensionless gas velocity is lower than 2, as shown in Fig. 5b, the coflowing gas

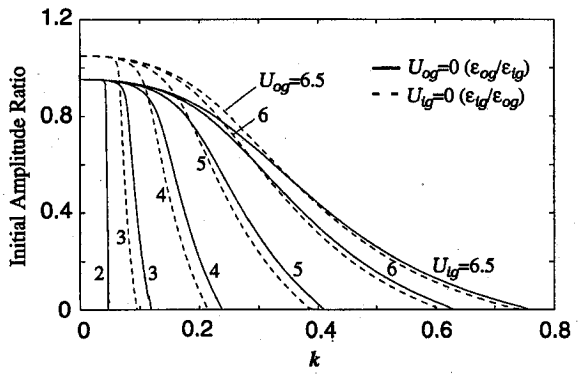

Fig. 4 Amplitude ratio of initial disturbances at the inner and outer interfaces for the parasinuous mode under the same conditions as in Fig. 3b.

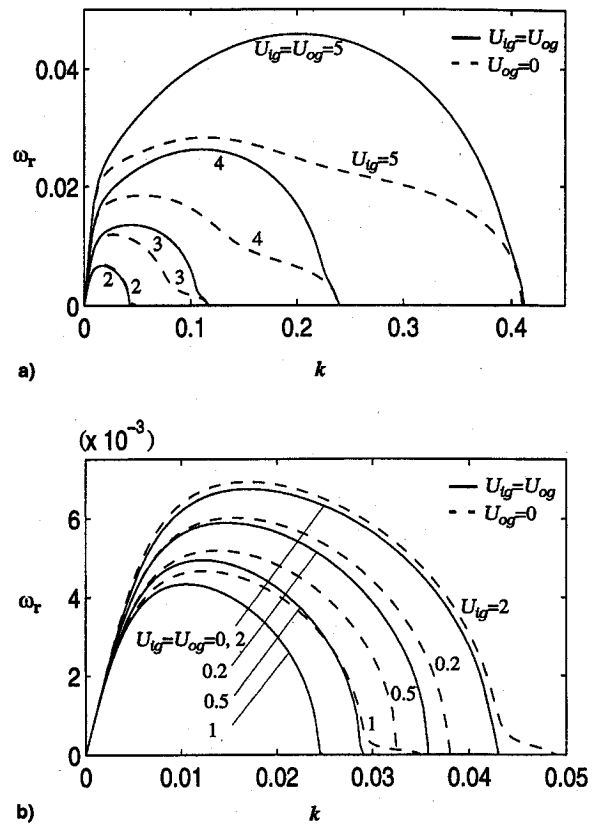

Fig. 5 Wave growth rate of the parasinuous mode for different velocities of gas streams on one side and both sides of the jet. a = 40.12, Re = 4112, We = 19.25, and ρ = 0.00129: a) high and b) low gas velocity.

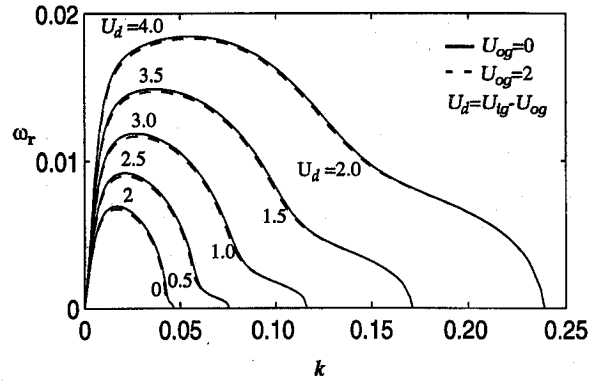

Fig. 6 Effects of velocity difference between inner and outer gas streams on the parasinuous wave growth rate for a = 40.12, Re = 4112, We = 19.25, and ρ = 0.00129.

stream has little effect on the wave growth rate. Hence, it is less attractive for practical applications at low gas velocities.

Shown in Fig. 6 is the wave growth rate with the same velocity jump across each interface, but distinct velocity difference ($U_d = U_{ig} - U_{og}$) between two gas streams for each pair of curves. It is seen that the growth rates for each pair of curves are almost the same, indicating that it is the velocity discontinuity across each interface that mainly determines the growth rate. The small difference shown is because of the different outer gas velocities ($U_{og} = 0$ for solid curves and $U_{og} = 2$ for dashed curves), implying also that the breakup of the annular liquid jet depends on not only the velocity difference across each interface, but also the absolute velocity of each liquid and gas stream. Similar effect of absolute velocity has been found for the instability and breakup of plane liquid sheets[13] and cylindrical liquid jets.[17] However, it should be

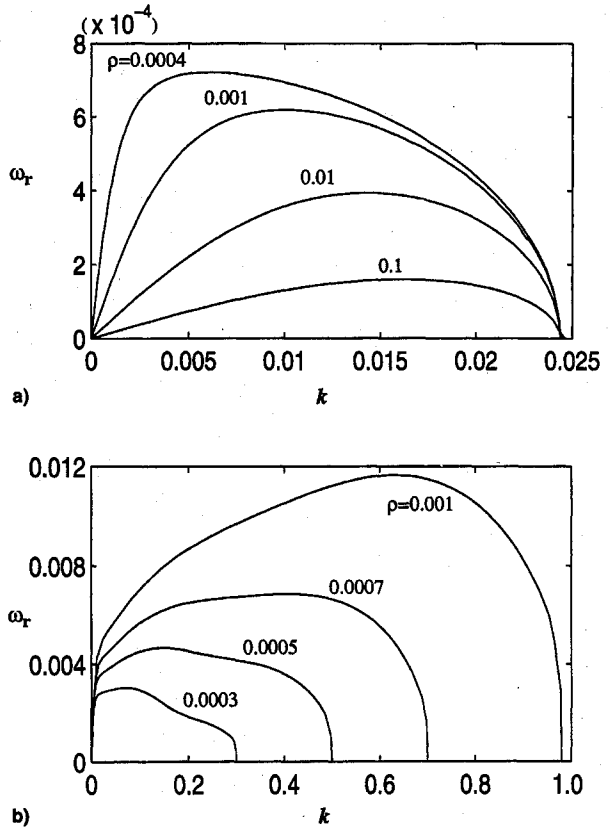

Fig. 7 Density effects on the parasinuous wave growth rate for a = 40.12, Re = 1000, and We = 1000: a) without velocity discontinuity, $U_{lg} = U_{og} = 1$ and b) with velocity discontinuity, $U_{lg} = 0$ and $U_{og} = 1$.

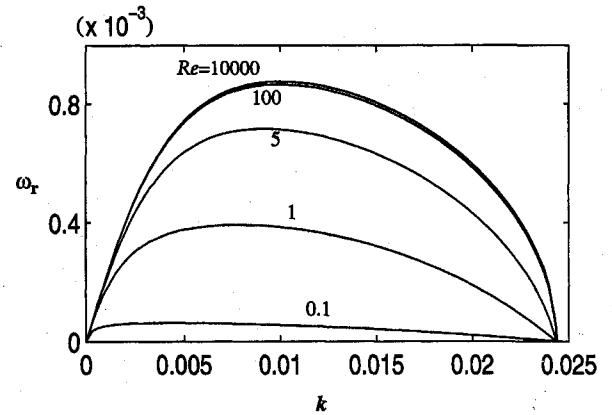

Fig. 8 Viscous effects of liquid on the parasinuous wave growth rate without velocity discontinuity. a = 40.12, We = 500, ρ = 0.001, and $U_{lg} = U_{og} = 1$.

pointed out that the effect of absolute velocity is relatively small and at best secondary, compared to that of velocity differences across the interfaces.

Effects of Various Flow Parameters

The parasinuous wave growth rates shown in Figs. 7–9 illustrate the effects of gas-to-liquid density ratio, liquid viscosity, and surface tension on the breakup process of an annular viscous liquid jet at fixed jet radii (a = 40.12 and b = 42.12).

Figure 7 shows the growth rate at Re = 1000, We = 1000, and different density ratios of gas-to-liquid. It is found that without velocity discontinuity at the gas–liquid interfaces (Fig. 7a), increasing liquid density or decreasing gas density promotes the jet breakup process, an effect opposite to the result

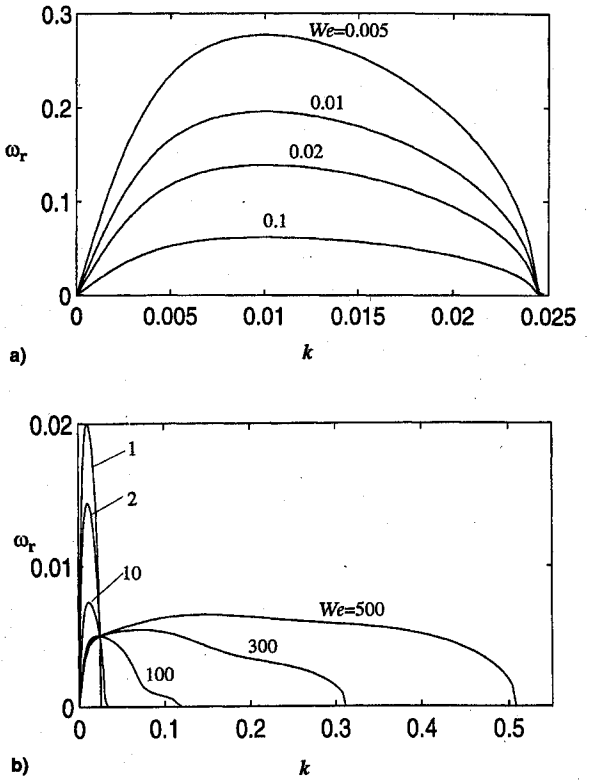

Fig. 9 Surface tension effects on the parasinuous wave growth rate for a = 40.12, Re = 1000, and ρ = 0.001: a) without velocity discontinuity, $U_{lg} = U_{og} = 1$ and b) with velocity discontinuity, $U_{lg} = 0$ and $U_{og} = 1$.

with the velocity discontinuity as shown in Fig. 7b. This implies that the presence of a gas medium would suppress the jet instability for the special case of $U_{ig} = U_{og} = 1$. However, it enhances the jet instability when there is a velocity difference between the liquid and gas phases,[5] as for a cylindrical liquid jet.[18]

To examine the viscous effects of liquid, the wave growth rate with various Reynolds number is presented in Fig. 8 for the Weber number of 500. The increase in growth rate with Reynolds number indicates that the liquid viscosity has a stabilizing effect on the jet instability, a trend also seen in cases with a velocity difference.[5] However, it was found that the liquid viscosity may enhance the instability of thin liquid sheets at low Weber numbers.[5,6]

Surface tension effect is examined by observing the growth rates shown in Fig. 9 at different Weber numbers. It is found that the surface tension has a destabilizing effect when there is no velocity difference between the liquid and gas phases (Fig. 9a). This means that without aerodynamic interaction, the capillary force is the only source of the jet instability, consistent with the observation for a cylindrical liquid column by Rayleigh.[19] However, it is observed that with a velocity difference across any interface, surface tension is the source of instability only at low Weber numbers (Fig. 9b). At high Weber numbers, the source of the jet instability is the aerodynamic interaction between the liquid and gas phases. This is because, as for Rayleigh instability,[19] surface tension has a destabilizing effect only for long wavelength disturbances. As Weber number increases, the unstable disturbances move into short wavelength range where the surface tension has a stabilizing effect. This indicates that in atomization processes that usually occur at high Weber numbers, the onset of atomization is primarily because of the aerodynamic interaction that leads to the pressure fluctuation, which in turn causes the resonant oscillation of capillary waves at the liquid–gas interfaces.[20]

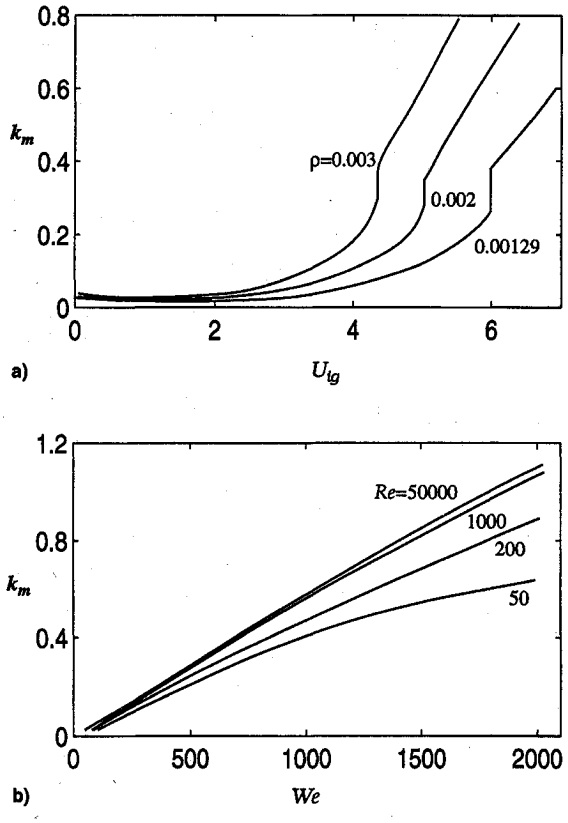

Fig. 10 Dominant wave number for the parasinuous mode with $a = 40.12$ and $U_{og} = 0$: a) $Re = 4112$, $We = 19.25$ and b) $\rho = 0.001$, $U_{lg} = 2$.

Dominant Wave Number

The dominant wave number k_m, for which the growth rate is a maximum, is important for practical applications, because it gives an indication of the ligament breakup length, and in the absence of secondary atomization, a direct link to the drop size of the resulting sprays. Therefore, the effect on k_m of various gas velocities, gas-to-liquid density ratios, Weber numbers, and Reynolds numbers has been investigated. The dependence of k_m on various flow parameters can also be seen partly from Figs. 2–9. For example, the dominant wave number in Fig. 3 decreases slowly for $U_{lg} < 1$ (or $U_{og} < 1$) and then increases quickly for $U_{lg} > 1$ (or $U_{og} > 1$) with U_{lg} (or U_{og}). Apparently, the surrounding gas streams with high velocities can improve the atomization performance in the sense of reducing the droplet sizes. There are no significant changes with the dominant wave number between the case of the gas stream inside of the liquid jet and that of the gas outside of the jet under the conditions considered, unlike wave growth rate. The coflowing gas streams increase the dominant wave number significantly when the dimensionless gas velocity is higher than 2 (see Fig. 5).

Further results concerning the dominant wave number are presented in Fig. 10. The wave number k_m is plotted with U_{lg} for three different density ratios ρ in Fig. 10a. It is seen that at a constant density ratio k_m decreases slightly first for $U_{lg} < 1$, and then increases with U_{lg} for $U_{lg} > 1$. Clearly, a minimum dominant wave number occurs at about $U_{lg} = 1$, showing that the droplet size may have a maximum if the gas velocity is the same as the jet velocity. When $U_{lg} > 1$, the dominant wave number increases smoothly with the gas velocity until a sudden increase in k_m at a fixed U_{lg}, e.g., $U_{lg} \approx 6$ for $\rho = 0.00129$, is reached. Beyond this point, the dominant wave number increases sharply with U_{lg}. The double value of k_m at certain U_{lg} and ρ suggests that broader distribution of droplet sizes in a spray may occur at a practical condition. It can also be seen from Fig. 10a that k_m always increases as the gas-to-liquid ρ increases, and the occurrence of the double-value k_m depends not only on the gas velocity, but also the density ratio, as shown in Figs. 3b and 7b. Therefore, it is the inertia of the gas stream that mainly affects the uniformity of droplet sizes in sprays.

Different from the effect of the gas inertia on k_m, *We* and *Re* exhibit monotonic influence on the dominant wave number. As shown in Fig. 10b, k_m increases with *We* for a constant *Re*, and increases also with *Re* at a fixed *We*. This indicates that both surface tension and liquid viscosity may reduce the dominant wave number. That is, the wavelength linked to the droplet size in liquid jet atomization may be increased, showing that to improve liquid atomization performance, less viscous liquid and small surface tension fluid should be utilized in practice.

Conclusions

A linear instability analysis has been carried out for an annular viscous liquid jet exposed to both inner and outer gas streams of unequal velocities. Muller's method is used to solve the dispersion relation for the temporal mode of unstable solutions. The results show that not only the velocity difference across each interface, but also the absolute velocity of each fluid phase is important for jet instability, although the effect of absolute velocity is secondary compared to that of relative velocity. Coflowing gas at high velocities is found to significantly improve atomization performance, while a low-velocity coflowing gas stream has little effect on jet instability when compared with the case where a gas stream of the same velocity is applied only on one side of the liquid jet. A high-velocity gas inside of the annular liquid jet promotes the jet breakup processes more than gas outside of the jet with equivalent velocity. For equal liquid and gas velocities, surface tension, liquid and gas density exhibit effects completely opposite to those with velocity discontinuity across interfaces. However, the viscous damping effect on jet instability always exists for the cases with and without the velocity differences at high Weber numbers. Atomization performance is enhanced by an increase in the liquid inertia, density ratio, and relatively large gas velocity, and hindered by the effect of surface tension and liquid viscosity.

Acknowledgments

The financial support of the Natural Sciences and Engineering Research Council of Canada and the University of Victoria, via a Graduate Fellowship awarded to the first author, is gratefully acknowledged.

References

[1]Lefebvre, A. H., *Atomization and Sprays*, Hemisphere, New York, 1990.

[2]Crapper, G. D., Dombrowski, N., and Pyott, G. A. D., "Kelvin-Helmholtz Wave Growth on Cylindrical Sheets," *Journal of Fluid Mechanics*, Vol. 68, Pt. 3, 1975, pp. 497–502.

[3]Meyer, J., and Weihs, D., "Capillary Instability of an Annular Liquid Jet," *Journal of Fluid Mechanics*, Vol. 179, June 1987, pp. 531–545.

[4]Lee, J. G., and Chen, L. D., "Linear Stability Analysis of Gas-Liquid Interface," *AIAA Journal*, Vol. 29, No. 29, 1991, pp. 1589–1595.

[5]Shen, J., and Li, X., "Instability of an Annular Viscous Liquid Jet," *Acta Mechanica*, Vol. 114, Nos. 1–4, 1996, pp. 167–183.

[6]Li, X., and Tankin, R. S., "On the Temporal Instability of a Two-Dimensional Viscous Liquid Sheet," *Journal of Fluid Mechanics*, Vol. 226, May 1991, pp. 425–443.

[7]Lin, S. P., and Creighton, B., "Energy Budget in Atomization," *Aerosol Science and Technology*, Vol. 12, 1990, pp. 630–636.

[8]Mansour, A., and Chigier, N., "Disintegration of Liquid Sheets," *Physics of Fluids*, Vol. 2, No. 5, 1990, pp. 706–719.

[9]Hashimoto, H., and Suzuki, T., "Experimental and Theoretical Study of Fine Interfacial Waves on Thin Liquid Sheet," *JSME Inter-*

national Journal, Ser. II34, 1991, pp. 277–283.

[10]Kendall, J. M., "Experiments on Annular Liquid Jet Instability and on the Formation of Liquid Shells," *Physics of Fluids*, Vol. 29, No. 7, 1986, pp. 2086–2094.

[11]Bers, A., "Space-Time Evolution of Plasma Instabilities-Absolute and Convective," *Handbook of Plasma Physics*, Vol. 1, 1983, pp. 452–517.

[12]Huerre, P., and Monkewitz, P. A., "Local and Global Instabilities in Spatially Developing Flows," *Annual Review of Fluid Mechanics*, Vol. 22, 1990, pp. 473–537.

[13]Li, X., "On the Instability of Plane Liquid Sheets in Two Gas Streams of Unequal Velocities," *Acta Mechanica*, Vol. 106, Nos. 1–4, 1994, pp. 137–156.

[14]Muller, D. E., "A Method for Solving Algebraic Equations Using an Automatic Computer," *Mathematical Tables and Aids to Computation*, Vol. 10, No. 5, 1956, pp. 208–215.

[15]Ramanurthi, K., and Tharakan, T. J., "Experimental Study of Liquid Sheets Formed in Coaxial Swirl Injectors," *Journal of Propulsion and Power*, Vol. 11, No. 6, 1995, pp. 1103–1109.

[16]Rangel, R. H., and Sirignano, W. A., "The Linear and Nonlinear Shear Instability of a Fluid Sheet," *Physics of Fluids A*, Vol. 3, No. 10, 1991, pp. 2392–2400.

[17]Li, X., and Shen, J., "Breakup of Cylindrical Liquid Jets in Co-Flowing Gas Streams," *Proceedings of Emerging Energy Technology Symposium, ASME Energy Week Conference and Exhibition* (Houston, TX), 1996, pp. 22–31.

[18]Lin, S. P., and Lian, Z. W., "Mechanisms of the Breakup of Liquid Jets," *AIAA Journal*, Vol. 28, No. 1, 1988, pp. 120–126.

[19]Rayleigh, L., "On the Instability of Jets," *London Mathematical Society*, Vol. 10, 1879, pp. 361–371.

[20]Lin, S. P., and Kang, D. J., "Atomization of a Liquid Jet," *Physics of Fluids*, Vol. 30, No. 7, 1987, pp. 2000–2006.